



This is a repository copy of *Removal of organic matter from reservoir water: mechanisms underpinning surface chemistry of natural adsorbents*.

White Rose Research Online URL for this paper:

<https://eprints.whiterose.ac.uk/131064/>

Version: Accepted Version

Article:

Hussain, S., van Leeuwen, J., Aryal, R. et al. (3 more authors) (2018) Removal of organic matter from reservoir water: mechanisms underpinning surface chemistry of natural adsorbents. *International Journal of Environmental Science and Technology*, 15 (4). pp. 847-862. ISSN 1735-1472

<https://doi.org/10.1007/s13762-017-1447-3>

Reuse

Items deposited in White Rose Research Online are protected by copyright, with all rights reserved unless indicated otherwise. They may be downloaded and/or printed for private study, or other acts as permitted by national copyright laws. The publisher or other rights holders may allow further reproduction and re-use of the full text version. This is indicated by the licence information on the White Rose Research Online record for the item.

Takedown

If you consider content in White Rose Research Online to be in breach of UK law, please notify us by emailing eprints@whiterose.ac.uk including the URL of the record and the reason for the withdrawal request.



eprints@whiterose.ac.uk
<https://eprints.whiterose.ac.uk/>

1 **Removal of organic matter from reservoir water: mechanisms underpinning surface**
2 **chemistry of natural adsorbents**

3 Short title: Fuller's earth for treating surface water

4

5 Sabir Hussain ^{a*}, John van Leeuwen ^{a,c}, Rupak Aryal ^a, Binoy Sarkar ^{c*}, Christopher W.K.
6 Chow ^{a,b}, Simon Beecham ^a

7

8 ^a Natural and Built Environments Research Centre, School of Natural and Built Environments,
9 University of South Australia, Mawson Lakes, SA 5095, Australia.

10 ^b Australian Water Quality Centre, South Australian Water Corporation, Adelaide, SA 5000,
11 Australia.

12 ^c Environmental Science and Engineering Strand, Future Industries Institute, University of South
13 Australia, Mawson Lakes, SA 5095, Australia.

14

15

16

17

18

19

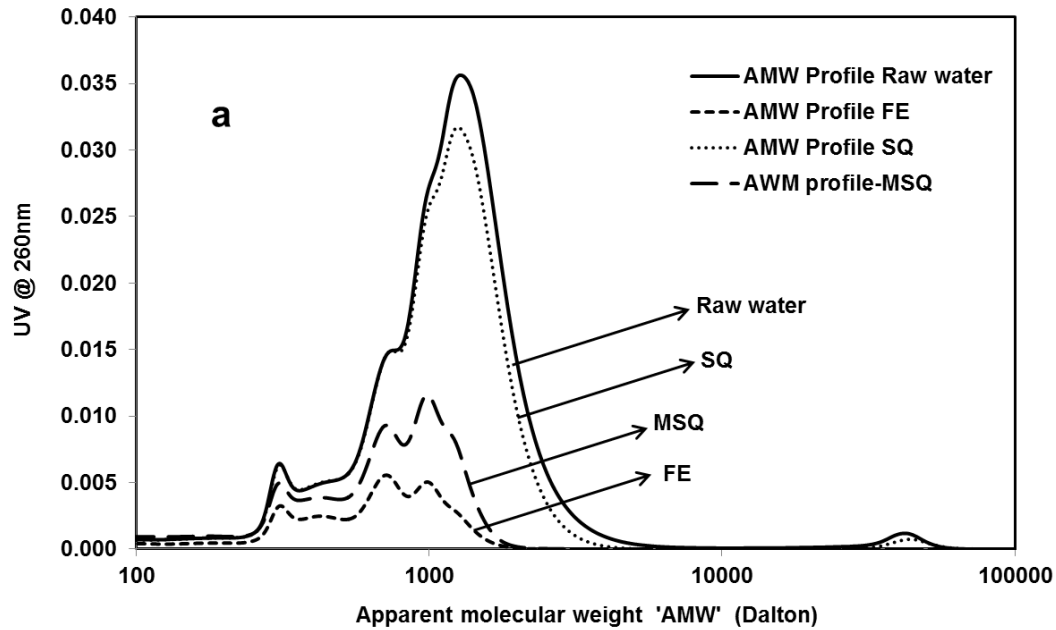
20 * Corresponding authors:

21 B. Sarkar; e-mail: binoy.sarkar@unisa.edu.au

22 S. Hussain; e-mail: sabir.hussain@mymail.unisa.edu.au

23 **Graphical abstract**

24



25

26

27 **Highlights**

- 28 • Fuller's earth (FE), natural and modified quartz were studied for DOC removal from reservoir
- 29 water.
- 30 • FE yielded greater DOC removal at broad range of pH and at low dose than quartz sand.
- 31 • F-EEM and HPSEC showed higher removal of humic substance and low AMW compounds.
- 32 • Adsorption data best fitted to Freundlich model, indicating multilayer adsorption.
- 33 • Pseudo-second-order kinetic model fitting indicated a chemisorption process.

34

35 **Abstract**

36 One of the key challenges in water treatment industry is the removal of organic compounds by
37 cost-effective methods. This study evaluated the adsorptive removal of dissolved organic carbon
38 (DOC) from reservoir water using fuller's earth (FE) in comparison with natural (SQ) and
39 modified quartz (MSQ) sands. The removal capacities of FE at different contact times, pH levels,
40 adsorbent dosages and initial DOC concentrations were compared with both the quartz sands.
41 The optimum DOC removals by FE and SQs were achieved at contact time of 60 min and 30
42 min, pH level of 6 and 4, and at adsorbent dose of 1.5 g/150 mL and 10 g/100 mL, respectively.
43 The adsorption capacity of FE (1.05 mg/g) was much higher compared to the MSQ (0.04 mg/g)
44 and SQ (0.01 mg/g). Adsorption equilibrium data better fitted to the Freundlich model than the
45 Langmuir model, suggesting that adsorption occurred primarily through multilayer formation
46 onto the surfaces of FE and SQ. The pseudo-second-order model described the uptake kinetics
47 more effectively than the pseudo-first-order and intra-particle diffusion models, indicating that
48 the mechanism was primarily governed by chemisorption. These observations were well
49 supported by the physiochemical characteristics and charge behaviour of the adsorbents. In
50 mass-transfer study, the results of liquid film diffusion model showed that the adsorption of
51 DOC on FE was not controlled by film diffusion, but other mechanisms also played an essential
52 role. This study demonstrates that FE is an effective adsorbent for the removal of DOC in surface
53 water treatment.

54

55 **Keywords:** Adsorption; Fluorescence spectroscopy; Isotherm and kinetics; Liquid film diffusion;
56 Water treatment.

57 **1. Introduction**

58 Dissolved organic matter (DOM) in natural waters is a complex heterogeneous mixture of
59 naturally occurring organic constituents such as humic and fulvic acids that are coloured,
60 aromatic and hydrophobic in nature. It also comprises of low molecular weight organics that are
61 hydrophilic in nature, including aliphatic and nitrogenous compounds such as amino acids,
62 carbohydrates and proteins (Matilainen et al. 2011). DOM, measured as dissolved organic carbon
63 (DOC) in surface waters, has increased considerably in the last couple of decades in many
64 regions of the world, likely because of the exacerbation of environmental issues such as global
65 warming, intensification of drought and rain events, and soil acidification (Forsberg 1992; Korth
66 et al. 2004; Worrall and Burt 2007). The presence of DOC in drinking water can cause
67 significant problems to water supply utilities because it can produce unpleasant colour, taste and
68 odour, and may act as substrate for microbial growth in distribution systems. It may increase
69 coagulant or disinfectant demands, foul membrane's surface and clog activated carbon pores,
70 which deteriorate the treatment performance. If not removed adequately by the treatment
71 process, higher levels of chlorine used for disinfection may react with residual DOC to form
72 disinfection by-products (DBPs) such as trihalomethanes (THMs), and these can be of serious
73 health concerns (Collins et al. 1986; Tang et al. 2016).

74 Traditionally, DOC removal from drinking water has been accomplished by coagulation (Deegan
75 et al. 2011; Hussain et al. 2014; Matilainen et al. 2010; Rahbar et al. 2006). However, more
76 recently, a shift is evident towards adsorption with activated carbon (Bonvin et al. 2016;
77 Dastgheib et al. 2004; Matilainen et al. 2006), ion-exchange resins (Arias-Paic et al. 2016;
78 Humbert et al. 2005; Kitis et al. 2007) and membrane filtration technologies (Van der Bruggen et
79 al. 2003; Yang et al. 2014). In coagulation, one of the main disadvantages is the handling of

80 sludge and its disposal. In addition, adsorption with activated carbon and use of membrane filters
81 are cost intensive; and desorption by ion-exchange resins also cause disposal problems for large
82 amounts of concentrated waste brine produced during the process. This showed that the removal
83 of organic matter by cost-effective methods is still one of the key challenges in water treatment
84 industry. As a result, efficient and cost effective adsorbents are actively sought by scientists and
85 water industries around the world. One of the main advantages of using natural or modified
86 adsorbents over traditional water purification methods is that these materials may be easily
87 regenerated and reused during the water treatment process (Chow et al. 2009).

88 Fuller's earth (FE), a natural clay material also known as 'bleaching earth', has been successfully
89 used for the removal of heavy metals (Oubagaranadin et al. 2007), bleaching of crude edible oil
90 (Mana et al. 2008), dyes (Atun et al. 2003) and polyvinylalcohol (Bajpai and Vishwakarma
91 2003) due to its low cost, high surface area and abundant availability. The current approaches are
92 well established with the use of activated carbon and anion exchange resins for DOM removal,
93 but the findings on the potential use of FE is still limited. The functional relationship between the
94 physiochemical characteristics of this natural adsorbent and plausible mechanism for DOC
95 removal is also largely unknown. Therefore, this work was emphasised on the potential
96 application of natural fuller's earth in surface water treatment. For this purpose, FE's results
97 were compared with the natural and modified quartz sands which were earlier reported as an
98 effective material for organic matter removal from water (Hedegaard and Albrechtsen 2014;
99 Jarvis and Majewski 2012). The present study was aimed (1) to examine the DOC removal
100 capacity of FE in comparison with SQs at different contact times, pH levels, adsorbent dosages
101 and initial DOC concentration, and (2) to empirically predict the mechanisms of DOC removal
102 by these adsorbents in relation to their physiochemical characteristics. This research was

103 conducted at the Natural and Built Environments Research Centre, School of Natural and Built
104 Environments, University of South Australia, Mawson Lakes, Australia during Oct 2014-May
105 2015.

106

107 **2. Materials and Methods**

108 2.1. Water collection and analysis

109 Water samples were collected from the inlet point of the water treatment plant of Myponga
110 Reservoir in South Australia. All samples were stored in a cold room at 4°C prior to the batch
111 experiments. DOC was measured using a total organic carbon analyser (Model 820, Sievers
112 Instruments Inc., USA). UV absorbance (at 254 nm) and true colour calibrated by 50 HU Cobalt
113 Platinum standards (at 456 nm) were determined using a UV-120 UV-Vis spectrophotometer
114 (MIOSTECH Pty Ltd., Australia). A portable pH meter (TPS, Model WP-91) was used to
115 measure the pH of raw and treated waters. The water quality was as follows: DOC, 12.5±0.2
116 mg/L; UV_{254nm}, 0.444±0.005/cm; specific UV absorbance (SUVA), 3.6 L/mg.m; colour, 43±2
117 HU; specific colour, 3.4; turbidity, 1.9±0.1 NTU; pH, 7.4±0.2 and alkalinity of the raw water,
118 108 mg/L as CaCO₃.

119 For DOM characterisation, high performance size-exclusion chromatography (HPSEC) and
120 fluorescence excitation-emission matrix (F-EEM) spectroscopy were employed. HPSEC
121 technique was used to determine the apparent molecular weight (AMW) profile of DOM present
122 in raw and treated waters as described by Chow et al. (2008). F-EEM spectra were acquired
123 using a Perkin–Elmer LS55 fluorescence spectrophotometer. The fluorescence intensities of
124 DOM composition corresponding to F-EEM regions I, II, III, IV and V, and referred to as
125 Protein 1 (P1), Protein 2 (P2), fulvic acid (FA), soluble microbial products (SMP) and humic

126 acid (HA) like compounds, respectively, were calculated adopting the method as described by
127 Chen et al. (2003). The sum (total) and mean fluorescence intensities of P1, P2, FA, SMP and
128 HA regions were determined based on the total number of data points (N) of these regions as
129 1000, 1000, 2880, 840 and 4800, respectively. The total fluorescence intensities of P1, P2, FA,
130 SMP and HA regions for the surface waters were about 109, 644, 3533, 268 and 3972 arbitrary
131 units (au), whereas the mean intensity values of the corresponding regions were about 0.1, 0.58,
132 1.27, 0.27 and 0.78 units, respectively. The higher fluorescence intensities of HA and FA-like
133 compounds indicated that the reservoir water was mainly comprised of humic substances. Gone
134 et al. (2009) also reported that these compounds (HA and FA) are the common fluorophores in
135 natural surface water.

136

137 2.2. Adsorbent characterisation

138 The FE and SQ were supplied by Ace Chemical Company and Unimin Australia Pty. Ltd.
139 (Adelaide, South Australia), respectively. Both adsorbents were oven dried at 50°C prior to the
140 adsorption study. The surfaces of SQ were modified with allylamine compound ($C_3H_5NH_2$) by
141 plasma polymerization method as discussed in (Jarvis and Majewski 2012). Therefore, the
142 modified SQ was named as MSQ. Das et al (2013) also reported similar approach for the
143 removal of perfluorooctane sulfonate compounds from water using oleylamine-modified clay
144 adsorbent. The structural and surface chemical characteristics of FE and SQs were determined
145 using scanning electron microscopy (SEM), Fourier transform infrared (FTIR) spectroscopy, and
146 thermo-gravimetric analysis (TGA). Surface area and pore size distribution were determined
147 using N_2 adsorption measurements at liquid nitrogen temperature by Gemini 2380 surface area
148 analyser (Micrometrics, USA) (Table 1). The SEM images of FE and SQs were taken in high

149 vacuum mode and with a 20kV accelerating voltage by an Everhart-Thornley Detector (ETD) or
150 Large Field Detector (LFD) using a FEI Quanta 450 FEG Environmental Scanning Electron
151 Microscope. The elemental composition of the samples were analysed by energy dispersive x-ray
152 spectroscopy (EDX) using an Apollo EDX detector (EDAX[®], USA).
153 For FTIR analysis, the samples were ground and mixed homogenously with dehydrated KBr and
154 pressed into discs. Infrared (IR) spectra were acquired using an Agilent Cary 600 Series FTIR
155 Spectrometer over spectrum wavenumbers 4,000-400 cm⁻¹. The spectrum range was obtained by
156 the co-addition of 64 scans with a resolution of 4 cm⁻¹. (Bajpai and Vishwakarma 2003) also
157 adopted a similar range of spectrum (4,000-400 cm⁻¹) in studying the adsorption of
158 polyvinylalcohol onto FE surfaces. Thermogravimetric analysis (TGA) was performed using a
159 Mettler-Toledo-TGA/DSC1 instrument (Mettler-Toledo International Inc.). The temperature for
160 TGA was raised from 25 to 900°C at a heating rate of 10°C/min with a resolution of 6°C under
161 N₂ flow (70 mL/min).

162

163 2.3. Batch experiments

164 Batch experiments of FE and SQs were conducted to study the effect of key parameters on the
165 DOC removal. This was done at the following experimental conditions: contact time: 2–240 min;
166 pH levels: 4–11; adsorbent doses: 0.05–15 g/150mL for FE and 1–40 g/100mL for SQs; and
167 initial DOC concentration: 6.8–80 mg/L. A series of conical flasks containing a known volume
168 of raw water were agitated at a pre-determined agitation speed of 300 rpm on an orbital shaker.
169 The desired concentration of DOC was acquired by adding fulvic acid (FA), supplied by Omnia
170 (Nutriology) Specialties Australia Pty Ltd, Australia, in tested surface waters. The FA used in
171 this study was extracted from a natural aged humus and concentrated into a completely soluble

172 dry powder which contains about 70% fulvic acid, 5% humic acid, 18% potassium and 4%
173 nutrients. The stock solution (2000 mg/L) of FA was prepared by dissolving 2 g of FA into 1 L
174 high purity Milli-Q water. The pH of tested water was adjusted by 0.2 M HCl or 0.2 M NaOH
175 solutions. For kinetic study, the time required for reaching the equilibrium condition was
176 determined by withdrawing the treated water samples of individual flask at different time
177 intervals. Immediately after this, the treated water samples were filtered through 11 µm
178 Whatman No. 1 filters, followed by 0.45 µm and 0.22 µm syringe filters. The filtrates were
179 further analysed for the measurement of final DOC, UV_{254nm} and colour. The percentage removal
180 of each parameter was determined using the following equation (Eq. 1):

$$181 \quad \text{Removal (\%)} = \frac{(C_i - C_e) \times 100}{C_i} \quad (\text{Eq. 1})$$

182 Where, C_i and C_e are the initial and final concentrations of water parameters (such as DOC in
183 mg/L), respectively.

184

185 2.4. Adsorption equilibrium and kinetic studies

186 Adsorption equilibria and rate data are the essential requirements in designing an adsorption
187 system. Adsorption studies were carried out by varying the adsorbent dosages at pre-determined
188 optimum conditions. The equilibrium adsorption capacities were evaluated at contact time higher
189 than 60 min, when the equilibrium condition was reached. The DOC adsorption data were
190 analysed by fitting to Langmuir, Freundlich, Temkin and Dubinin-Redushkevich models. The
191 linear equations of these models were used to assess the best-fit model and to determine the
192 adsorption mechanisms of DOC as either monolayer or multilayer formation onto the adsorbent
193 surfaces. The suitability of each model was determined by linear regression (comparison of

194 coefficient of determination, R^2) from the experimental data. The equilibrium adsorption
195 capacity or q_e (mg/g) was calculated as follows (Eq. 2):

$$196 \quad q_e = \frac{(C_i - C_e) \cdot V}{m} \quad (\text{Eq. 2})$$

197 Where, C_i and C_e are the initial and final concentration of DOC (mg/L), V is the volume of
198 surface water (mL) and m is the mass of adsorbent (g).

199 Kinetics of DOC adsorption by FE, MSQ and SQ were investigated as a function of time by four
200 different kinetics models, i.e., pseudo-first-order, pseudo-second-order, intra-particle diffusion
201 and liquid film diffusion model. The coefficient of determination values of each model were
202 obtained from the linear plots. The experimental q_e values of pseudo-first-order and pseudo-
203 second-order models were compared with the calculated q_e values to assess the best fit model.

204

205 **3. Results and Discussion**

206 3.1. Physiochemical characteristics of adsorbents

207 The SEM micrographs of FE, MSQ and SQ were shown in Fig. 1. The outer surface of all three
208 adsorbents show crystalline forms with honeycomb apertures. However, the FE images exhibited
209 greater surface area and porous surfaces than the SQs. The particle morphology of FE was more
210 irregular and comprised aggregates of microcrystalline plates while the surfaces of SQs were less
211 irregular and towards singular (not aggregate) particle. The FTIR spectra of the adsorbents are
212 shown in Fig. 2. The IR spectra of FE exhibited broad bands at about 1000 cm^{-1} and 3500 cm^{-1} ,
213 indicating the presence of both free and hydrogen bonded OH groups (Socrates, 2004). These
214 spectra mark the presence of silanols with Si-O stretching and aluminols with Al-O stretching at
215 1000 cm^{-1} and 3500 cm^{-1} in FE (Gu et al., 2011). In addition, the strong band at around 1700 cm^{-1}
216 1 of the spectra also indicates the presence of carboxylate anion and asymmetrical stretching of

217 C=O. However, FTIR spectra for SQs showed weak bands at 3500 cm⁻¹ and strong bands at 1000
218 cm⁻¹, indicating lack of Al-O stretching as observed in FE. The peaks at around 775 cm⁻¹ and 795
219 cm⁻¹ are doublets of quartz which show Si-O stretching (Perelomov et al. 2016). In addition, Fig.
220 2 showed the clear doublet for sands, but not for FE because quartz contents in FE are less than
221 SQ. The SEM-EDX elemental analysis showed that the FE was mainly composed of O (50.2%),
222 C (21.7%), Si (15.5%), Al (7.2%), Ca (2.4%), Na (2.7%) and others (0.4%), whereas, the SQs
223 were mainly composed of Si (65-67%), O (32-35%) and Al (0.3-0.4%). TGA curves of the FE,
224 MSQ and SQ were used to quantify the weight loss with increasing temperature. The first weight
225 loss at around 100-115°C corresponded to the dehydration of physical water present in all
226 adsorbents. The second weight loss in FE at 500°C might be due to the loss of organic content
227 present in the adsorbent itself. The sharp weight loss of MSQ at 280°C was probably due to the
228 loss of its polymerized allylamine coating from the material's surface (Sarkar et al., 2010a;
229 2010b). It was also observed that both SQ (after 110°C) and MSQ (after 280°C) slightly gained
230 some weight with increasing temperature, reflecting possible oxide formation.

231

232 3.2. Process parameters for DOC removal

233 3.2.1 *Effect of contact time*

234 The effect of different contact times on adsorptive removal of DOC using 1g/150mL of FE and
235 5g/100mL of SQs at neutral pH are shown in Fig.3. In the case of FE, it was evident that there
236 was a rapid removal of DOC within the first few minutes and the equilibrium was reached at a
237 contact time of 60 min, after which the removals of UV_{254nm} and colour and DOC remained
238 unchanged. The initial rapid adsorption followed a very slow approach to equilibrium, and
239 therefore, contact time of 60 min was considered as optimum time. The removal efficiencies at

240 contact time of 60 min were about 43%, 64% and 85% for DOC, UV_{254nm} and colour,
241 respectively. These were significantly higher than the removals of these components by SQ (6%,
242 10% and 13%, respectively) and MSQ (19%, 17% and 38%, respectively) at a contact time of 30
243 min, which was found to be the optimum contact time for both sands. Based on these results, the
244 subsequent experiments were conducted using 60 and 30 min contact times for FE and SQs,
245 respectively.

246

247 3.2.2. *Effect of initial pH*

248 The removal of DOC was examined over a pH range of 4-11 (Fig. 4). Adsorption characteristics
249 of the adsorbents were highly pH dependent. The results show that the percentage removal of
250 DOC was decreased as the initial pH of water solution increased. This was likely because the
251 adsorbent surfaces at pH < 7 became more positively charged due to protonation, leading to the
252 adsorption of negatively charged DOC on the FE's surface at lower pH conditions. Such
253 protonation reactions commonly occur on mineral surfaces having variable charges (Rusmin et
254 al. 2016; Sarkar et al. 2011). The maximum adsorptive removals for FE were achieved over a pH
255 range 4–6. The final pH levels of the treated waters were in the range of 3.4–3.8. The optimum
256 pH for DOC removal by FE was determined to be at pH 6, at which more than 90% of colour,
257 55% of DOC and 73% of UV_{254nm} were removed. FE had almost no effect on the removal of
258 DOC and colour at pH > 9. Removal of DOC by FE was near to zero or negative at highly
259 alkaline conditions (pH ≥ 10), also indicating at high pH, the solubilisation of particulate organic
260 matter had occurred or naturally occurring organic matter present on/in the adsorbent material
261 got desorbed into the aqueous phase. At this high pH, the variably charged adsorbent surface also
262 became negatively charged as a result of deprotonation (Rusmin et al. 2016; Sarkar et al. 2011),

263 which consequently would impart a repulsive force to the negatively charged DOC molecules
264 and decrease adsorption capacity. In addition, the TGA results of FE (Fig. 2) showed that there
265 was significant weight loss at temperatures between 400 and 500°C, which might be partially
266 due to the loss of organic matter present within the FE. To confirm this, 1 g of FE was agitated in
267 150 mL solution of high purity Milli-Q water at pH 11 for 1 h. DOC concentration in the clear
268 supernatant was found to be approximately 4.3 mg/L. Also, the EEM spectra of this solution
269 confirmed the presence of high fluorescence intensities of FA and HA compounds (figure not
270 shown). The above results clearly showed that at high pH conditions (≥ 10), FE did not adsorb
271 DOC.

272 The zeta potential and electrophoretic mobility values of FE decreased significantly from +0.8 to
273 -41 mV and -1.2 to -3.3 $\mu\text{m}\cdot\text{cm}/\text{Vs}$, when the pH was increased from 1 to 11. The point of zero
274 charge (pzc) or isoelectric point (IEP) of both FE and SQ were near to pH 2.0 and 5.1,
275 respectively. The IEP values of the SQs used in this study were previously documented by
276 (Jarvis and Majewski 2012). They reported that IEP of MSQ increased by modifying the surface
277 of SQ. In general, the adsorbent surface was positively charged at pH below the IEP whereas the
278 surfaces were generally negatively charged at pH above the IEP. For SQs, the maximum
279 removals of DOC, colour and $\text{UV}_{254\text{nm}}$ were achieved at pH 4, thus the optimum pH for both
280 quartz sands was chosen as pH 4. The removals achieved by SQs were much lower in
281 comparison to the removal achieved by FE. Subsequent experiments were conducted at pH 6 for
282 FE and at pH 4 for SQs.

283

284 *3.2.3. Effect of adsorbent dose*

285 The effects of adsorbent dose on the removals of DOC, colour and UV_{254nm} are shown in Fig. 5.
286 FE was used at dosages ranging from 50 mg-15 g/150 mL while SQs were used at levels
287 between 1-40 g/100 mL. The increase in the FE dose up to 1.5 g FE/150 mL surface water
288 resulted in rapid increase in DOC removal, but at higher dose, further removals were minimal,
289 indicating equilibrium condition had been reached. At 1.5 g/150 mL of FE, the removals of
290 DOC, colour and UV_{254nm} were found to be 56%, 94% and 79%, respectively. At this dose, the
291 specific UV absorbance (SUVA) value of treated water decreased to 1.8 L/mg.m from the initial
292 value of 3.6 L/mg.m, indicating most of the hydrophobic compounds were removed by FE. In
293 case of SQs, a dose between 5 -10 g/100 mL surface water was required to achieve the maximum
294 DOC removal (Fig. 5b). For SQ, the removal efficiencies of DOC, colour and UV_{254nm} were
295 approximately 14%, 37% and 17%, whereas for MSQ these values were approximately 31%,
296 70% and 29%, respectively. The SUVA values of treated waters were found to be more than 3.2
297 at all dosages, indicating that treated water was still hydrophobic in nature. Thus, the DOC
298 removal achieved by FE was significantly greater than the SQs. For subsequent experiments, the
299 FE dose of 1.5g /150 mL and, 10 g/100 mL dose of SQs were chosen as optimum dosages.

300

301 3.2.4. *Effect of initial DOC concentration*

302 DOC removal efficiencies gradually decreased when the initial DOC concentration was
303 increased for all adsorbents tested at their optimum dosages (Fig. 6). The results showed that the
304 dose of 3 g/150 mL of FE was able to remove about 90% of colour, 80% of UV_{254nm} and more
305 than 70% of DOC even at the initial DOC concentrations exceeding 25 mg/L. This probably
306 occurred as a result of decrease in adsorbate to adsorbent ratio, resulting in the increase of
307 available number of surface sites for adsorption. Comparatively, DOC removals achieved by SQs

308 were very low when initial DOC concentration exceeded 20 mg/L, with removal efficiencies
309 below 20%.

310

311 3.3. DOM characterisation in treated water

312 F-EEM spectroscopy was employed to evaluate the DOM composition of raw and treated waters.

313 The EEM spectra of five regions, P1, P2, FA, SMP and HA (as detailed in Section 2.1) are
314 shown in Fig. 7. Total fluorescence intensities (FI) of P1, P2, FA, SMP and FA for the FE treated

315 water were about 80, 314, 996, 131 and 773 units, respectively. For MSQ, the corresponding

316 total FI were about 24, 256, 2548, 130 and 2904 units, whereas for SQ, intensities were about 35,

317 304, 2724, 144 and 3168 units, respectively. In addition, the mean FI of P1, P2, FA, SMP and

318 HA for the FE treated water were about 0.07, 0.28, 0.32, 0.13 and 0.15 units, respectively. For

319 MSQ, the corresponding mean FI were about 0.02, 0.23, 0.81, 0.13 and 0.57 units, whereas for

320 SQ, these were about 0.03, 0.27, 0.87, 0.15 and 0.63 units, respectively. The above results

321 indicate that the mean FI of P1, P2 and SMP of treated waters for the three adsorbents tested

322 were almost the same compared to the mean FI of FA and HA. Gone et al. (2009) demonstrated a

323 linear relationship between the different fluorescence peak (namely A, C and T) intensities and

324 DOC percentage removal, and found that the decrease in organic matter fluorescence intensity

325 can be used as a simple technique for the prediction of DOC removal (Gone et al. 2009). The

326 maximum removals of total FI of HA and FA achieved by FE were 86% and 71% compared to

327 the removals achieved by MSQ (27% and 28%) and SQ (20% and 23%), respectively. The

328 results showed that the FE yielded higher removal of humic acids-like compounds whereas SQs

329 yielded higher removals of proteins-like compounds (P1 and P2) than the FE.

330 The selective removals of organic compounds of specific apparent molecular weights (AMW)
331 were determined by partitioning the AMW profile into four zones, Zone 1 (100-500 Da), Zone 2
332 (500-2,000 Da), Zone 3 (2,000-10,000 Da) and Zone 4 (10,000-70,000 Da). The relative
333 abundances of organics with AMWs within zones 1, 2, 3 and 4 in raw water were 11.2%, 75.3%,
334 10.8% and 2.7%, respectively. This indicates that organics in the AMW range of 600-2,000 Da
335 were the most dominant in raw water. Each adsorbent showed different removal efficiency at its
336 particular optimum condition. The HPSEC results indicate that FE can remove between ~ 50
337 to 100% of UV absorbing organic compounds in the range of 100–70,000 Da, whereas the
338 removal rates of MSQ and SQ for the same range of AMW were ~13–100% and ~0.3–55%,
339 respectively, depending on the molecular weight (Fig. 8). This indicates that FE is more efficient
340 for the removal of low molecular weight organic compounds than MSQ, and SQ shows the
341 lowest removals for all zones.

342 3.4. Adsorption isotherms

343 Isothermal modelling is commonly employed to relate the capacity of adsorbate removal by the
344 adsorbent and to describe the mechanisms by which adsorption occurs at the interface. The
345 adsorption experimental data were analysed using linear forms of Langmuir, Freundlich, Temkin
346 and Dubinin-Redushkevich (D-R) isotherm models, based on the linearized coefficient of
347 determination (Supplementary Information: Fig. S1). The Langmuir model assumes that the
348 adsorption occurs primarily by saturated monolayer formation of the adsorbate on the surface of
349 adsorbent with no lateral interaction between the adsorbed molecules, and is based on surface
350 homogeneity having equal energy. The Langmuir equation (Langmuir 1918) is expressed as (Eq.
351 3):

$$352 \quad q_e = \frac{abC_e}{1+aC_e} \quad (\text{Eq. 3})$$

353 The linear form of the Langmuir isotherm model is (Eq. 4):

$$354 \quad \frac{1}{q_e} = \frac{1}{abC_e} + \frac{1}{b} \quad (\text{Eq. 4})$$

355 Where, q_e is the adsorption capacity (mg/g); a (L/mg) is the Langmuir constant and is indirectly
356 related to the enthalpy of adsorption; b (mg/g) is the maximum sorption capacity for monolayer
357 coverage of the adsorbent, and C_e (mg/L) is the equilibrium concentration of adsorbate in the
358 solution. The values of a and b were determined from the slope and intercept of plot of $1/q_e$ vs.
359 C_e (Supplementary Information: Fig. S1a). The Langmuir constant ‘ a ’ value of FE was greater
360 than the SQs, which indicated the affinity of FE towards DOC. *However*, the negative values of
361 the Langmuir constants ‘ a ’ and ‘ b ’ (Table 2) reflected the inadequacy of this isotherm model for
362 describing the adsorption process despite it showed a considerable linearity for data fitting
363 (correlation coefficient, R^2 ranging from 0.68 to 0.98). *Additionally*, a dimensionless constant,
364 separation factor or equilibrium parameter, R_L (Eq. 5), was calculated using the Langmuir
365 constant and was used to determine the adequacy or inadequacy of this model.

$$366 \quad R_L = \frac{1}{1+aC_i} \quad (\text{Eq. 5})$$

367 Where, ‘ C_i ’ is the initial concentration of DOC, and ‘ a ’ is the Langmuir constant. The R_L values
368 between 0 to 1, 0 and > 1 indicate favourable, irreversible and unfavourable adsorption,
369 respectively (Fierro et al., 2008; Bhatt et al., 2012). In the current study, R_L values of FE and SQ
370 were > 1 . *The negative value of ‘ a ’* for DOC adsorption onto FE yielded the R_L value > 1
371 (unfavourable adsorption). This further showed the inadequacy of fitting of the Langmuir model
372 to the adsorption data.

373 The Freundlich model (Freundlich 1926) is employed to describe surface heterogeneity, and can
374 be expressed as (Eq. 6):

375
$$q_e = K_f C_e^{1/n} \quad (\text{Eq. 6})$$

376 The linear form of above equation is (Eq. 7):

377
$$\log q_e = \log K_f + \frac{1}{n} \log C_e \quad (\text{Eq. 7})$$

378 Where, K_f (mg/g) is the Freundlich affinity coefficient and refers to the adsorption capacity and
379 n (dimensionless) is the Freundlich exponential coefficient, whose value can depend on
380 adsorbent types and experimental pH values. Generally, the adsorption strength increases as the
381 value of n decreases and the adsorption capacity decreases as K_f decreases (Hyung and Kim
382 2008). The values of K_f and n were determined from the plot of $\log q_e$ vs. $\log C_e$ (Supplementary
383 Information: Fig. S1b). In this study, the n and K_f values of FE were much greater than both SQs
384 (Table 2). The Freundlich and Langmuir isotherm models' parameters and correlation
385 coefficients values of FE, MSQ and SQ were given in Table 2. The Langmuir constant 'a' value
386 of FE was greater than the SQs, which described as an indication of the affinity of FE towards
387 DOC. The adsorption data of FE closely fitted to the Freundlich model ($R^2 = 0.99$), followed by
388 Langmuir model ($R^2 = 0.98$).

389 Temkin model is used to determine the heat of adsorption and the adsorbent-adsorbing species
390 interactions. Temkin model can be expressed as follows (Eq. 8):

391
$$q_e = \frac{RT}{b} \ln(K_T C_e) \quad (\text{Eq. 8})$$

392 The linearized form of above equation is (Eq. 9):

393
$$q_e = B_1 \ln K_T + B_1 \ln C_e \quad (\text{Eq. 9})$$

394 Where, B_1 is related to heat of adsorption which is equal to RT/b ; R Universal gas constant
395 (8.314 J/mol.K); T absolute temperature (K). The constants B_1 and K_T (L/mg) were determined
396 from the plot of q_e vs. $\ln C_e$ (Supplementary Information: Fig. S1c). The values of B_1 for FE and

397 MSQ were found to be 4.40 and 1.89, respectively whereas the K_T values for FE and MSQ were
398 found to be 0.20, and 3.72, respectively. It was observed from the values of B_I and K_T that heat of
399 adsorption for FE is greater than MSQ whereas the binding energy for FE is lower than MSQ.

400 Dubinin-Redushkevich (D-R) adsorption isotherm is expressed as follows (Eq. 10):

$$401 \quad q_e = q_m \exp(-Be^2) \quad (\text{Eq. 10})$$

402 The linear form of the D-R equation is (Eq. 11):

$$403 \quad \ln q_e = \ln q_m - Be^2 \quad (\text{Eq. 11})$$

404 Where, q_m is the theoretical monolayer saturation capacity (mg/g); e is known as Polanyi
405 potential and is equal to $e = RT \ln(1 + \frac{1}{c_e})$. B is the constant of free adsorption energy (mg^2/J^2)
406 and E is the apparent adsorption energy (J/mg) which was calculated using the following
407 formula; $E=1/\sqrt{2B}$. The value of E was derived from the slope and intercept of e^2 and $\ln q_e$
408 (Supplementary Information: Fig. S1d). Results obtained from the linear plot showed that the
409 value of mean free energy E of adsorption per molecule of adsorbate for FE (223.6 J/mg) was
410 much higher than MSQ (100 J/mg) and SQ (50 J/mg).

411 *Overall, the R^2 value of Freundlich model for FE and MSQ was comparatively greater than the*
412 *R^2 values of Langmuir, Temkin and D-R isotherm models which explained multilayer*
413 *adsorption. These adsorption data suggested that DOC adsorption occurred primarily by*
414 *multilayer formation in arbitrary distribution due to heterogeneous energetic distribution of*
415 *active sites onto the FE and SQs surfaces.*

416

417 3.5. Adsorption kinetics

418 The adsorption kinetics of DOC by FE and SQs were investigated from the pseudo-first-order,
419 pseudo-second-order and intra-particle diffusion models. The pseudo-first-order kinetic model

420 assumes that the rate of change in adsorbate uptake is directly related to the difference in the
421 saturation and the amount of solute uptake in a given time, and models the rate of adsorption of
422 adsorbate onto the adsorbent (Lagergren 1898). This model was expressed in a linear form as
423 (Eq. 12):

$$424 \quad \log(q_e - q_t) = \log q_e - k_1 t \quad (\text{Eq. 12})$$

425 Where, q_e and q_t are the adsorption capacity (mg/g) of the adsorbent at equilibrium and agitation
426 time t (min), respectively and k_1 is the pseudo-first-order rate constant (min^{-1}). The values of q_e
427 and k_1 were obtained from a linear plot of $\log(q_e - q_t)$ against contact time t (min), figure is not
428 shown here. The pseudo-second-order kinetic model proposed by (Ho and McKay 2000)
429 assumes that the chemisorption is the rate-limiting step, where the adsorption is due to physico-
430 chemical interaction. The linear form of this model is expressed as follows (Eq. 13):

$$431 \quad \frac{t}{q_t} = \frac{1}{k_2 q_e^2} + \frac{1}{q_e t} \quad (\text{Eq. 13})$$

432 Where, k_2 (g (mg min)^{-1}) is the pseudo-second-order rate constant and all other parameters are
433 the same as detailed in Equation 12. The values of q_e and k_2 were obtained from the linear plot of
434 t/q_t versus agitation time (Supplementary Information: Fig. S2a). The intraparticle diffusion
435 model assumes that the adsorption process is diffusion-controlled and that the rate of adsorption
436 depends on the speed at which adsorbate diffuses towards the adsorbent which is *expressed in*
437 *linear form using the following equation (Eq. 14):*

$$438 \quad q_t = k_3 t^{1/2} + C \quad (\text{Eq. 14})$$

439 Where, k_3 (g (mg/min)) is the intraparticle diffusion rate constant and C is the intercept. A linear
440 plot of q_t versus $t^{1/2}$ was used to obtain the values of k_3 and C (figure not shown).

441 The kinetic parameters determined for pseudo-first-order, pseudo-second-order and intra-particle
442 diffusion models, and the corresponding coefficient of determination for the adsorption of DOC
443 by FE, MSQ and SQ were presented in Table 2. The parameter values for each model indicate
444 that the adsorption rate was very fast for FE than the SQs. The results of pseudo-first-order
445 kinetic model indicated that the values of equilibrium adsorption capacities, q_e , did not agree
446 with the monolayer capacities determined by Langmuir equilibrium isotherm model and that the
447 plot of $\log(q_e - q_t)$ against *time* (t) was not truly linear, suggesting that the adsorption process did
448 not follow pseudo-first-order kinetics. When kinetic parameters along with R^2 for the pseudo-
449 second-order kinetic model were investigated, the agreement between experimental and
450 calculated equilibrium adsorption capacities, q_e , was evident. The plot of t/q_t versus agitation
451 time was highly linear and the R^2 value was very close to one. The experimental data was well
452 agreed with the pseudo-second-order model. The electrostatic attraction between the charged
453 surface of both adsorbents and DOM particles may be considered as the main adsorption
454 mechanism, suggesting DOC adsorption onto the adsorbents surfaces followed chemisorption
455 (Ho and McKay 2000; Rusmin et al. 2015).

456 When the intra-particle diffusion model was investigated, the regression of q_t versus $t^{1/2}$ was not
457 found to be linear and failed to pass through the origin. Instead, the plot reflected a large
458 intercept, suggesting greater boundary layer effect and contribution of the surface sorption in the
459 rate controlling step. These findings indicated that the intra-particle diffusion was not the sole
460 rate limiting step for the adsorption kinetics. The values of K_3 of this model for FE were greater
461 than SQs (Table 2). Furthermore, in mass-transfer study, the liquid film diffusion model,
462 (Oubagaranadin et al. 2007), was applied to determine the transfer behaviour of DOC molecule
463 to the solid phase boundary using the following equation (Eq. 15):

464
$$\ln (1 - F) = -K_{fd} t \quad (\text{Eq. 15})$$

465 Where, F is the ratio of q_t/q_e and K_{fd} is the film diffusion rate constant. The parameters of this
466 equation are similar to Equation 11 (pseudo-first-order kinetics). The results obtained from the
467 linear plot (Supplementary Information: Fig. S2b) between $-\ln (1-F)$ vs. *time* (t), indicating that
468 the straight lines of liquid film diffusion line for FE and SQs did not pass through the origin
469 (zero) point. This indicates that the adsorption system for FE and SQs was not mainly controlled
470 by film diffusion and a number of other mechanisms might play an essential role in controlling
471 the rate (Oubagaranadin et al. 2007).

472 FE has been widely used for bleaching and deodorization in food and petroleum industries such
473 as bleaching of crude edible oil in the refining process (Mana et al. 2008). With this benefit, FE
474 may have potential to be used for enhanced DOC removal through a hybrid treatment process
475 where the FE can be applied after coagulation by Al-based coagulants at pH range between 5-6
476 or by Ti and Zr-based coagulants at pH range between 3-5 (Hussain et al. 2014). The practicality
477 of using FE in such a hybrid system, at much lower concentration, is a subject for further
478 investigation.

479

480 **4. Conclusions**

481 In this study, the ability of low cost FE adsorbent to remove DOC in drinking water was
482 investigated and compared against DOC removal capabilities of MSQ and SQ. Experimental
483 results showed that FE could be highly effective for the removal of DOC. The major advantage
484 of DOC adsorption with FE was significant proportion of DOC removal at the lower dose tested
485 and at a pH level very close to neutral whereas both quartz sands performed better at a higher
486 dose and acidic pH conditions. A higher dose of FE (3 g/150 mL) showed potential to

487 consistently adsorb about 70% DOC even at the maximum DOC concentration of about 40
488 mg/L. EEM and HPSEC results confirmed that FE demonstrated greater removal of humic
489 compounds and low-high molecular weight compounds than SQs. The Freundlich model fitted
490 well to the adsorption data, indicating the DOC adsorption followed multi-layer formation onto
491 the FE and SQ surfaces. The adsorption kinetics was best described by the pseudo-second-order
492 model, suggesting removal mechanism followed chemisorption. Overall, the results of the
493 present study showed that FE is capable of greater DOC adsorption over a pH range 4 to 6 and at
494 comparatively low adsorbent dose over the SQs. This study demonstrates that FE is an effective
495 adsorbent for the removal of DOC in surface water treatment. Further research is suggested to
496 assess the prospective use of modified FE by thermal or chemical methods for its potential
497 application in water treatment.

498

499 **Acknowledgements**

500 The authors would like to thank the Australian Research Council (ARC) for providing financial
501 support for this research project, under grant LP110200208. The authors would also like to thank
502 Prof. Peter Majewski and his team of Mawson Institute, University of South Australia for
503 providing the natural and modified quartz sands.

504

505 **References**

506 Arias-Paic M, Cawley KM, Byg S, Rosario-Ortiz FL (2016) Enhanced DOC removal using
507 anion and cation ion exchange resins. *Water Research* 88:981-989
508 doi:<http://dx.doi.org/10.1016/j.watres.2015.11.019>

509 Atun G, Hisarli G, Sheldrick WS, Muhler M (2003) Adsorptive removal of methylene blue from
510 colored effluents on fuller's earth. *Journal of Colloid and Interface Science* 261:32-39
511 doi:[http://dx.doi.org/10.1016/S0021-9797\(03\)00059-6](http://dx.doi.org/10.1016/S0021-9797(03)00059-6)

512 Bajpai AK, Vishwakarma N (2003) Adsorption of polyvinylalcohol onto Fuller's earth surfaces.
513 *Colloids and Surfaces A: Physicochemical and Engineering Aspects* 220:117-130
514 doi:[http://dx.doi.org/10.1016/S0927-7757\(03\)00073-6](http://dx.doi.org/10.1016/S0927-7757(03)00073-6)

515 Bhatt AS, Sakaria PL, Vasudevan M, Pawar RR, Sudheesh N, Bajaj HC, Mody HM (2012)
516 Adsorption of an anionic dye from aqueous medium by organoclays: equilibrium
517 modeling, kinetic and thermodynamic exploration. *RSC Advances* 2: 8663-8671

518 Bonvin F, Jost L, Randin L, Bonvin E, Kohn T (2016) Super-fine powdered activated carbon
519 (SPAC) for efficient removal of micropollutants from wastewater treatment plant
520 effluent. *Water Research* 90:90-99 doi:<http://dx.doi.org/10.1016/j.watres.2015.12.001>

521 Chen W, Westerhoff P, Leenheer JA, Booksh K (2003) Fluorescence Excitation–Emission
522 Matrix regional integration to quantify spectra for dissolved organic matter.
523 *Environmental Science and Technology* 37:5701-5710 doi:10.1021/es034354c

524 Chow CWK, Majewski P, Bauer S, Fabris R, Drikas M (2009) Removal of natural organic
525 matter using self-assembled monolayer technology. *Desalination and Water Treatment*
526 12:344-351

527 Chow CWK, Fabris R, Leeuwen Jv, Wang D, Drikas M (2008) Assessing natural organic matter
528 treatability using high performance size exclusion chromatography. *Environmental*
529 *Science and Technology* 42:6683-6689 doi:10.1021/es800794r

530 Collins MR, Amy GL, Steelink C (1986) Molecular weight distribution, carboxylic acidity, and
531 humic substances content of aquatic organic matter: implications for removal during
532 water treatment. *Environmental Science and Technology* 20:1028-1032

533 Dastgheib SA, Karanfil T, Cheng W (2004) Tailoring activated carbons for enhanced removal of
534 natural organic matter from natural waters. *Carbon* 42:547-557
535 doi:<http://dx.doi.org/10.1016/j.carbon.2003.12.062>

536 Deegan AM, Shaik B, Nolan K, Urell K, Oelgemöller M, Tobin J, Morrissey A (2011)
537 Treatment options for wastewater effluents from pharmaceutical companies International.
538 *Journal of Environmental Science and Technology* 8:649-666 doi:10.1007/bf03326250

539 Fierro V, Torne-Fernandez V, Montane D, Celzard A (2008) Adsorption of phenol onto activated
540 carbons having different textural and surface properties. *Microporous and Mesoporous*
541 *Materials* 111:276-284

542 Forsberg C (1992) Will an increased greenhouse impact in Fennoscandia give rise to more humic
543 and coloured lakes? *Hydrobiologia* 229:51-58 doi:10.1007/BF00006990

544 Freundlich H (1926) *Colloid and capillary chemistry*. Methuen, London

545 Gone DL, Seidel J-L, Batiot C, Bamory K, Ligban R, Biemi J (2009) Using fluorescence
546 spectroscopy EEM to evaluate the efficiency of organic matter removal during
547 coagulation–flocculation of a tropical surface water (Agbo reservoir). *Journal of*
548 *Hazardous Materials* 172:693-699 doi:<http://dx.doi.org/10.1016/j.jhazmat.2009.07.052>

549 Hedegaard MJ, Albrechtsen H-J (2014) Microbial pesticide removal in rapid sand filters for
550 drinking water treatment – Potential and kinetics. *Water Research* 48:71-81
551 doi:<http://dx.doi.org/10.1016/j.watres.2013.09.024>

552 Ho YS, McKay G (2000) The kinetics of sorption of divalent metal ions onto sphagnum moss
553 peat. *Water Research* 34:735-742 doi:[http://dx.doi.org/10.1016/S0043-1354\(99\)00232-8](http://dx.doi.org/10.1016/S0043-1354(99)00232-8)

554 Humbert H, Gallard H, Suty H, Croué J-P (2005) Performance of selected anion exchange resins
555 for the treatment of a high DOC content surface water. *Water Research* 39:1699-1708
556 doi:<http://dx.doi.org/10.1016/j.watres.2005.02.008>

557 Hussain S, van Leeuwen J, Chow CWK, Aryal R, Beecham S, Duan J, Drikas M (2014)
558 Comparison of the coagulation performance of tetravalent titanium and zirconium salts
559 with alum. *Chemical Engineering Journal* 254:635-646
560 doi:<http://dx.doi.org/10.1016/j.cej.2014.06.014>

561 Hyung H, Kim J-H (2008) Natural organic matter (NOM) adsorption to multi-walled carbon
562 nanotubes: Effect of NOM characteristics and water quality parameters. *Environmental*
563 *Science and Technology* 42:4416-4421 doi:10.1021/es702916h

564 Jarvis KL, Majewski P (2012) Plasma polymerized allylamine coated quartz particles for humic
565 acid removal. *Journal of Colloid and Interface Science* 380:150-158
566 doi:<http://dx.doi.org/10.1016/j.jcis.2012.05.002>

567 Kitis M, İlker Harman B, Yigit NO, Beyhan M, Nguyen H, Adams B (2007) The removal of
568 natural organic matter from selected Turkish source waters using magnetic ion exchange
569 resin (MIEX®). *Reactive and Functional Polymers* 67:1495-1504
570 doi:<http://dx.doi.org/10.1016/j.reactfunctpolym.2007.07.037>

571 Korth A, Fiebiger C, Bornmann K, Schmidt W (2004) NOM increase in drinking water
572 reservoirs-relevance for drinking water production. *Water Supply* 4:55-60

573 Lagergren S (1898) Zur Theorie der Sogenannten Absorption gelöster Stoffe. PA Norstedt &
574 söner,

575 Langmuir I (1918) The adsorption of gases on plane surfaces of glass, mica and platinum.
576 Journal of the American Chemical Society 40:1361-1403 doi:10.1021/ja02242a004

577 Matilainen A, Gjessing ET, Lahtinen T, Hed L, Bhatnagar A, Sillanpää M (2011) An overview
578 of the methods used in the characterisation of natural organic matter (NOM) in relation to
579 drinking water treatment. Chemosphere 83:1431-1442
580 doi:<http://dx.doi.org/10.1016/j.chemosphere.2011.01.018>

581 Matilainen A, Vepsäläinen M, Sillanpää M (2010) Natural organic matter removal by
582 coagulation during drinking water treatment: A review. Advances in Colloid and
583 Interface Science 159:189-197 doi:<http://dx.doi.org/10.1016/j.cis.2010.06.007>

584 Matilainen A, Vieno N, Tuhkanen T (2006) Efficiency of the activated carbon filtration in the
585 natural organic matter removal. Environment International 32:324-331
586 doi:<http://dx.doi.org/10.1016/j.envint.2005.06.003>

587 Oubagaranadin JUK, Sathyamurthy N, Murthy ZVP (2007) Evaluation of Fuller's earth for the
588 adsorption of mercury from aqueous solutions: A comparative study with activated
589 carbon. Journal of Hazardous Materials 142:165-174
590 doi:<http://dx.doi.org/10.1016/j.jhazmat.2006.08.001>

591 Perelomov L, Sarkar B, Rahman MM, Goryacheva A, Naidu R (2016) Uptake of lead by Na-
592 exchanged and Al-pillared bentonite in the presence of organic acids with different
593 functional groups. Applied Clay Science 119, Part 2:417-423
594 doi:<http://dx.doi.org/10.1016/j.clay.2015.11.004>

595 Rahbar MS, Alipour E, Sedighi RE (2006) Color removal from industrial wastewater with a
596 novel coagulant flocculant formulation. International Journal of Environmental Science
597 and Technology 3:79-88 doi:10.1007/bf03325910

598 Rusmin R, Sarkar B, Biswas B, Churchman J, Liu Y, Naidu R (2016) Structural, electrokinetic
599 and surface properties of activated palygorskite for environmental application. *Applied*
600 *Clay Science* doi: 10.1016/j.clay.2016.07.012
601 doi:http://dx.doi.org/10.1016/j.clay.2016.07.012

602 Rusmin R, Sarkar B, Liu Y, McClure S, Naidu R (2015) Structural evolution of chitosan–
603 palygorskite composites and removal of aqueous lead by composite beads. *Applied*
604 *Surface Science* 353:363-375 doi:http://dx.doi.org/10.1016/j.apsusc.2015.06.124

605 Sarkar B, Megharaj M, Xi Y, Naidu R (2011) Structural characterisation of Arquad® 2HT-75
606 organobentonites: Surface charge characteristics and environmental application. *Journal*
607 *of Hazardous Materials* 195:155-161
608 doi:http://dx.doi.org/10.1016/j.jhazmat.2011.08.016

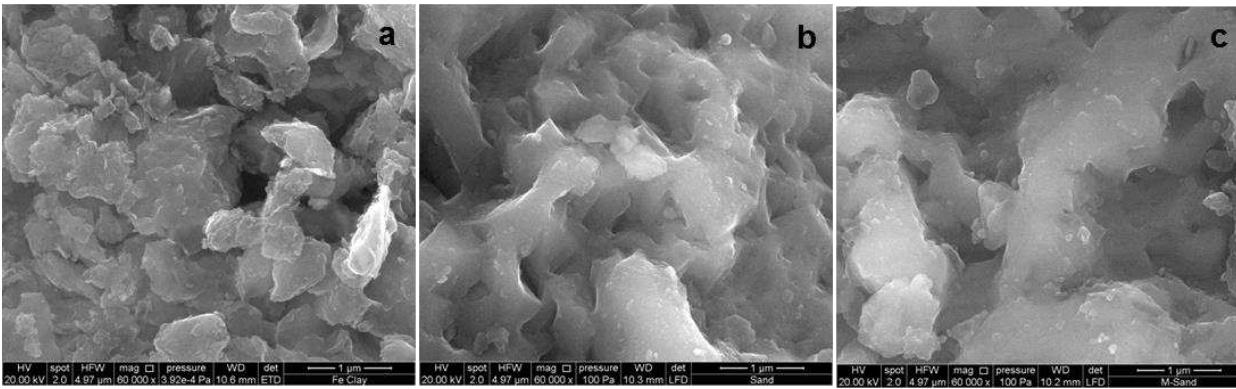
609 Tang Y, Xu Y, Li F, Jmaiff L, Hrudey SE, Li X-F (2016) Nontargeted identification of peptides
610 and disinfection byproducts in water. *Journal of Environmental Sciences* 42:259-266
611 doi:http://dx.doi.org/10.1016/j.jes.2015.08.007

612 Van der Bruggen B, Vandecasteele C, Van Gestel T, Doyen W, Leysen R (2003) A review of
613 pressure-driven membrane processes in wastewater treatment and drinking water
614 production. *Environmental Progress* 22:46-56

615 Worrall F, Burt TP (2007) Trends in DOC concentration in Great Britain. *Journal of Hydrology*
616 346:81-92 doi:http://dx.doi.org/10.1016/j.jhydrol.2007.08.021

617 Yang Y, Lohwacharin J, Takizawa S (2014) Hybrid ferrihydrite-MF/UF membrane filtration for
618 the simultaneous removal of dissolved organic matter and phosphate. *Water Research*
619 65:177-185 doi:http://dx.doi.org/10.1016/j.watres.2014.07.030
620

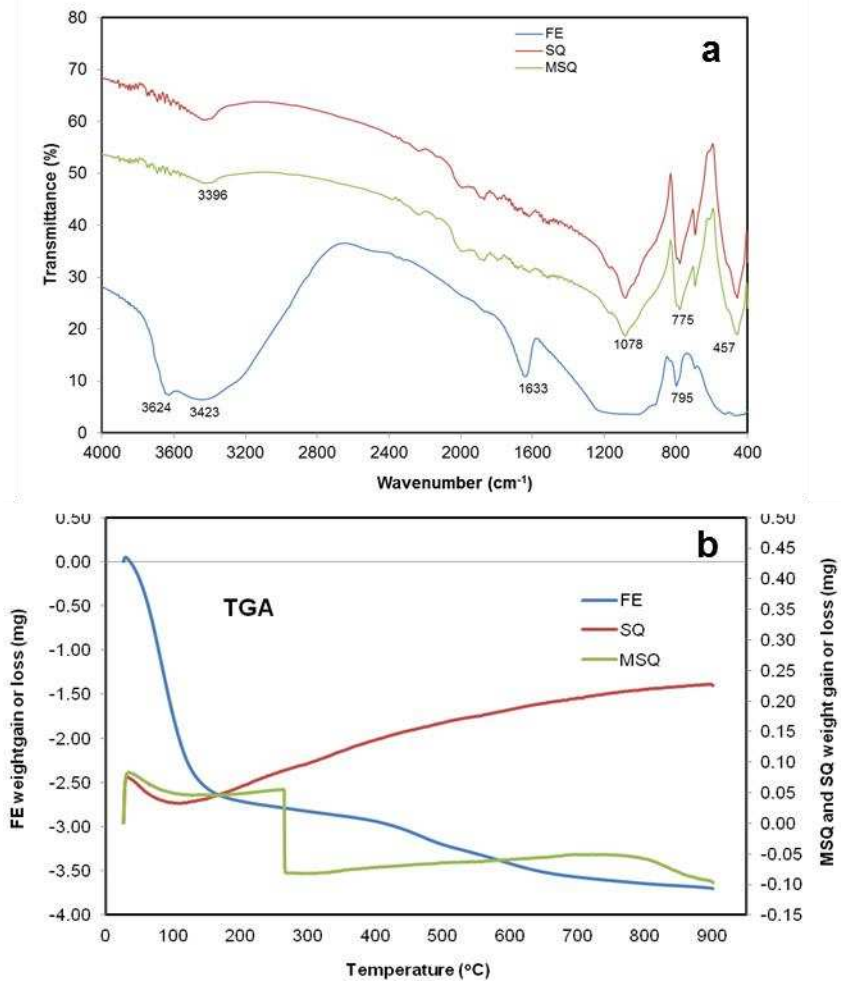
621 **Figures**



622 **Fig. 1.** SEM images of (a) fuller's earth, (b) quartz sand and (c) modified quartz sand.

623

624



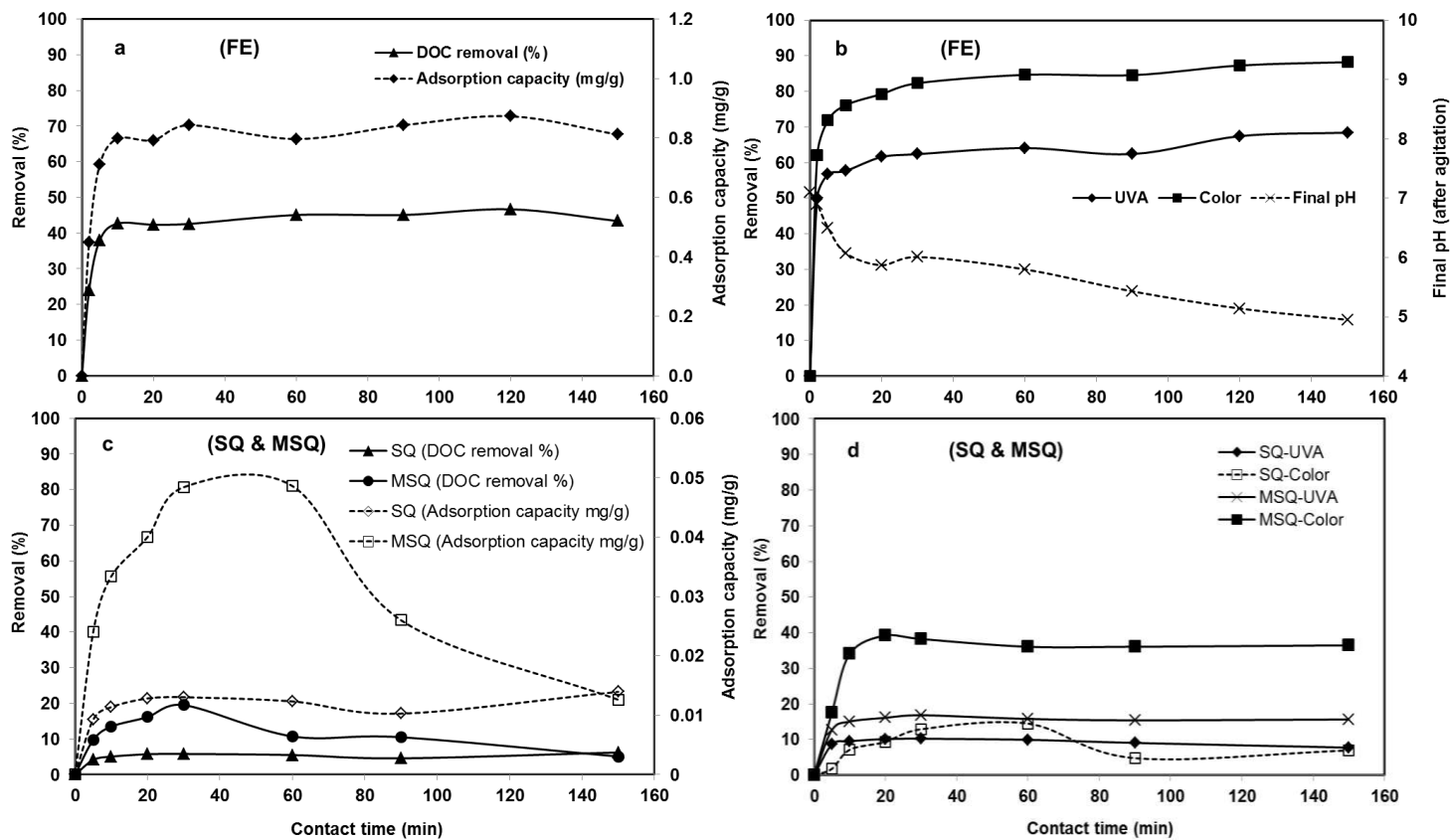
625

626 **Fig. 2.** FTIR spectra (a) and TGA plots (b) of fuller's earth (FE), quartz sand (SQ) and modified
 627 quartz sand (MSQ).

628

629

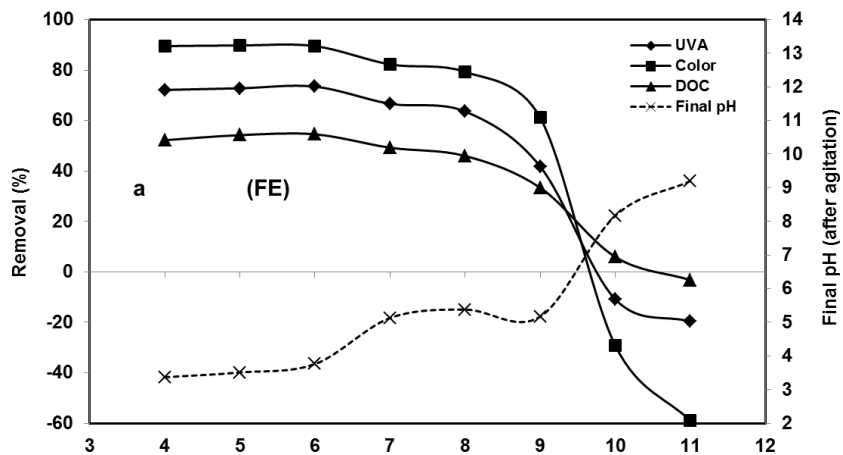
630



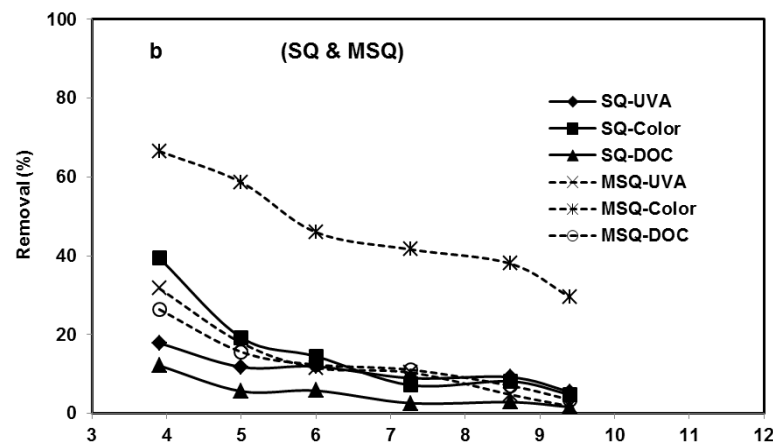
631

632 **Fig. 3.** Effect of contact time on the removal of DOC by (graphs a & b) fuller's earth (FE), and (graphs c & d) quartz sand with (MSQ)
633 or without (SQ) modification. Experimental conditions: contact time range = 0-150 min; adsorbent dose = 1 g for FE and 5 g for SQs;
634 agitation speed = 300 rpm.

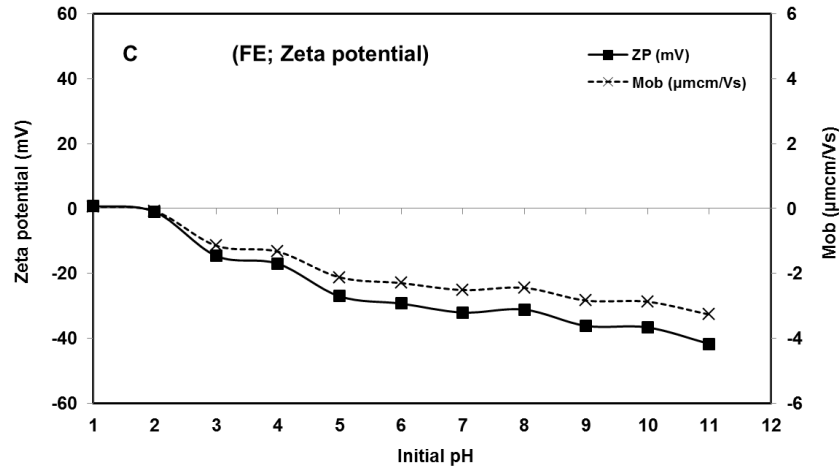
635



636

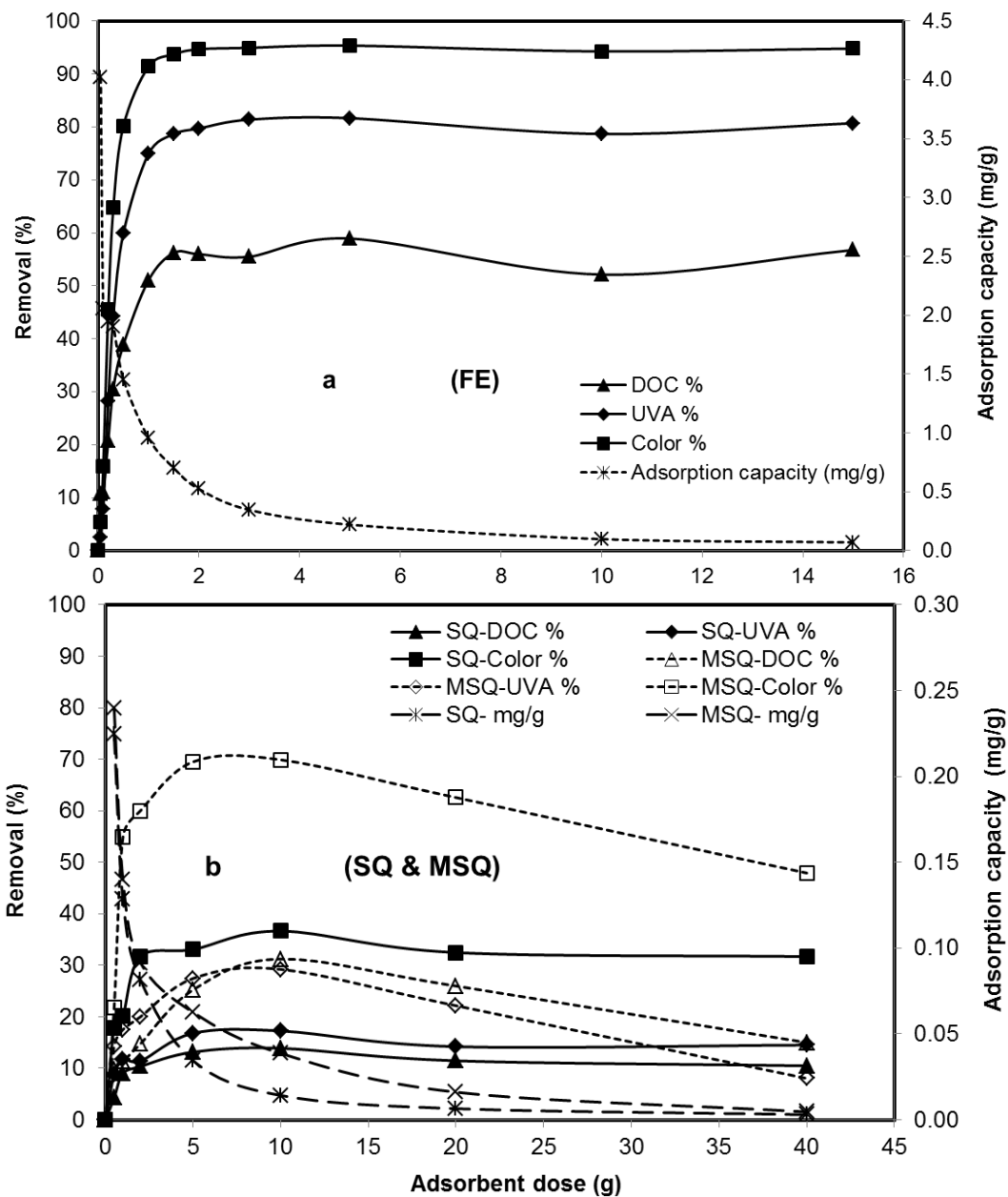


637



638

639 **Fig. 4.** Effect of pH on the removal of DOC by (a) fuller's earth (FE), (b) quartz sand with
640 (MSQ) or without (SQ) modification, and (c) pH-zeta potential relationship in fuller's earth
641 aqueous suspension. Experimental conditions: pH = 1-11; contact time = 60 min for FE and 30
642 min for SQs; adsorbent dose = 1 g for FE and 5 g for SQs; agitation speed = 300 rpm.

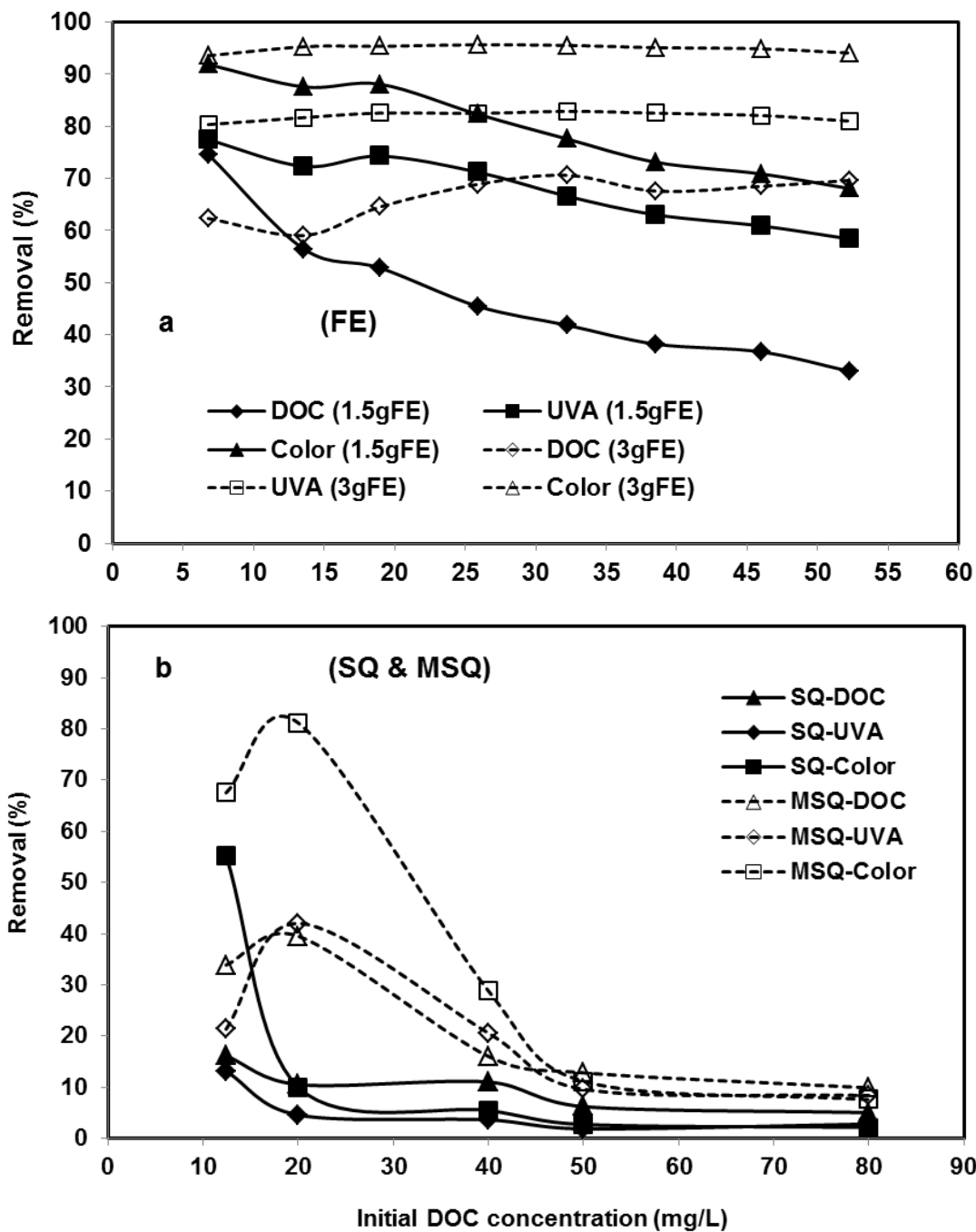


643

644

645 **Fig. 5.** Effect of adsorbent dose on the removal of DOC by (a) fuller's earth (FE), and (b) quartz
 646 sand with (MSQ) or without (SQ) modification. Experimental conditions: adsorbent dose = 0.05-
 647 15 g for FE and 0.5-40 g for quartz sand; contact time = 60 min for FE and 30 min for SQs; pH =
 648 6 for FE and 4 for SQs; agitation speed = 300 rpm.

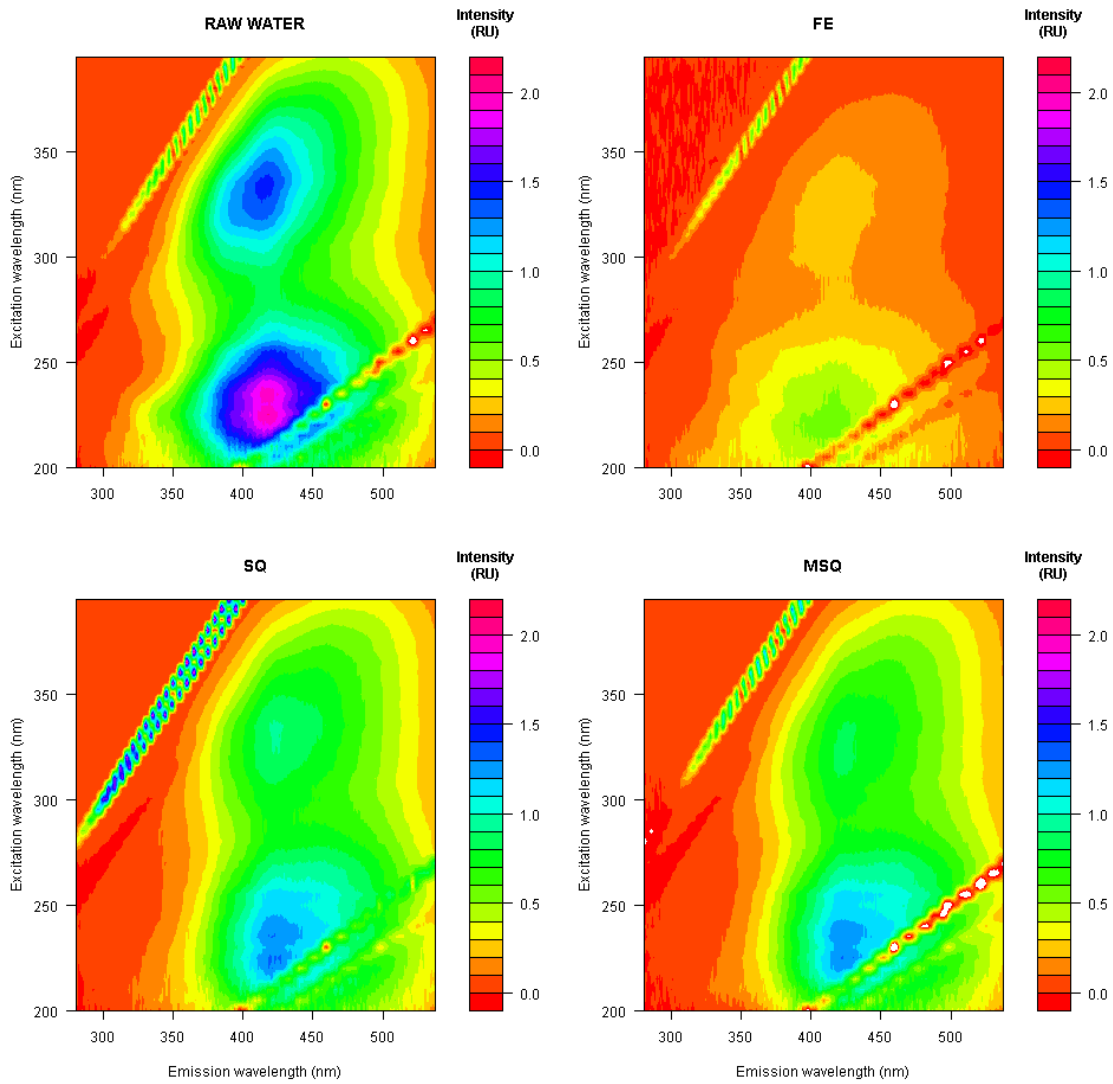
649



650

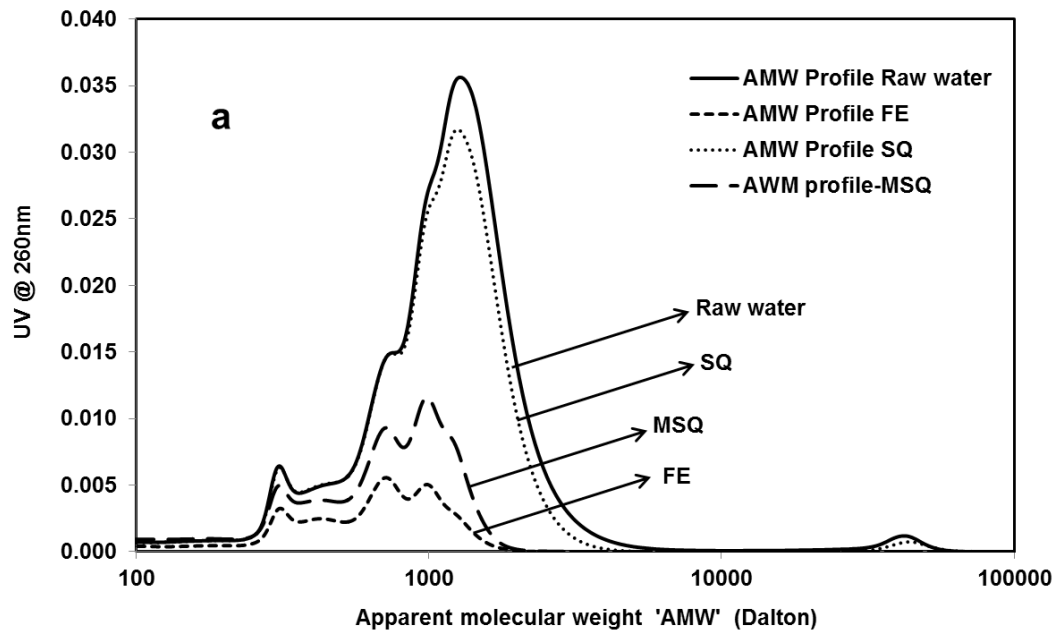
651

652 **Fig. 6.** Effect of initial adsorbate concentration on the removal of DOC by (a) fuller's earth (FE),
 653 and (b) quartz sand with (MSQ) or without (SQ) modification. Experimental conditions: contact
 654 time = 60 min for FE and 30 min for SQs; pH = 6 for FE and 4 for SQs; adsorbent dose = 1.5 g
 655 for FE and 10 g for SQs; agitation speed = 300 rpm.

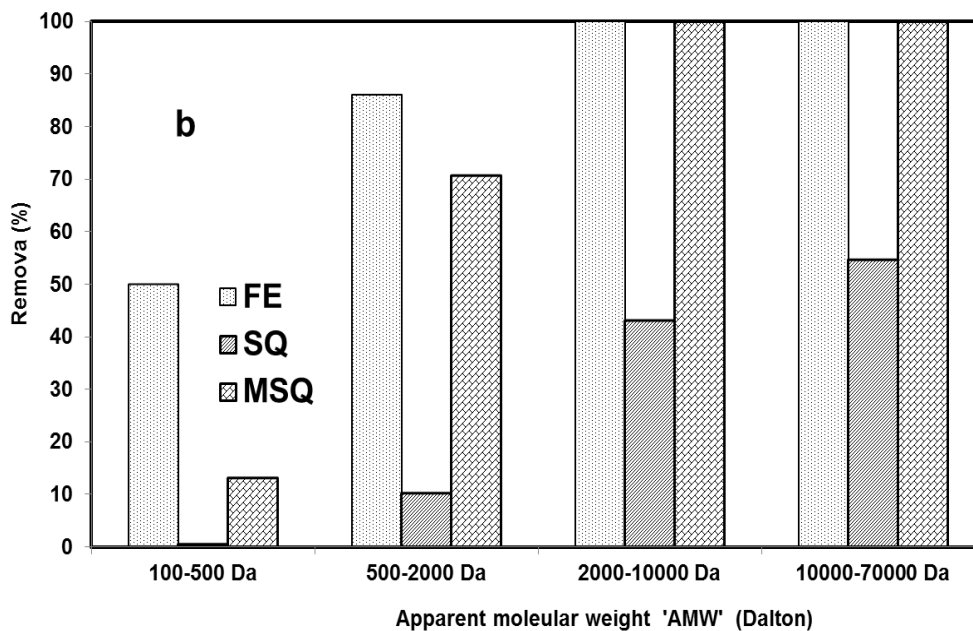


656 **Fig. 7.** 3D-fluorescence excitation-emission matrix (F-EEM) spectra of water samples before
 657 (raw) and after treatment with fuller's earth (FE) and quartz sand with (MSQ) or without (SQ)
 658 modification.

659



660



661

662 **Fig. 8.** High performance size-exclusion chromatography (HPSEC) based apparent molecular
 663 weight (AMW) profiles of water samples before (raw) and after treatment with fuller's earth
 664 (FE) and quartz sand with (MSQ) or without (SQ) modification: (a) reduction of UV 260 nm
 665 intensity, and (b) removal efficiencies.

666

667 **Tables**

668 **Table 1.** Physiochemical properties of fuller's earth (FE), quartz sand (SQ) and modified quartz
669 sand (MSQ).

Parameters	FE	SQ	MSQ
Surface areas			
Single point surface area at $P/P_0 = 0.30$; m^2/g	227.5	0.16	0.17
BET surface area; m^2/g	232.4	0.18	0.21
Langmuir Surface Area; m^2/g	364.4	0.30	0.38
Pore volume			
Single point adsorption total pore volume of pores less than 27.210 Å diameter at $P/P_0 = 0.300072359$; cm^3/g	0.115468	0.000079	0.000088
Pore size			
Adsorption average pore width (4V/A by BET); Å	19.87	18.05	17.04
Loose bulk density; g/L	462-550		
Free moisture; (2h, 110°C) %	13.7-15		
pH (10% suspension)	2.6-3.0		
Acid content as H_2SO_4 ; %	0.3-0.4	-	-
Loss on ignition; %	6-7		
Loose bulk density; g/L	462		
Residue > 63 µm (%)	9-35		
Particle size; µm	60-149	430	430

670

671

672 **Table 2.** Isothermal and kinetic model parameters for the adsorption of DOC on fuller's earth (FE), modified (MSQ) and natural (SQ) quartz
 673 sands.

Isotherm models												
Adsorbent	Freundlich model			Langmuir model			Temkin model			Dubinin-Redushkevich model		
	K_f (L/mg)	n	R^2	b (mg/g)	a (L/mg)	R^2	B_1	K_T	R^2	E (J/mg)	B (mg ² /J ²)	R^2
FE	1.25×10^{-2}	0.42	0.99	-1.1320	-0.0723	0.98	4.40	0.20	0.90	223.6	0.00001	0.93
MSQ	2.13×10^{-7}	0.18	0.89	-0.0178	-0.081	0.96	1.89	3.72	0.81	100.0	0.00005	0.87
SQ	2.99×10^{-20}	0.05	0.76	-0.0036	-0.092	0.68	4.25	0.15	0.52	50.0	0.00020	0.89

Kinetic models									
Adsorbent	q_e (exp) (mg/g)	Pseudo-first-order model			Pseudo-second-order model			Intra-particle diffusion	
		q_e (cal) (mg/g)	R^2	K_1 (min) ⁻¹	q_e (cal) (mg/g)	R^2	K_2 (g (mg min) ⁻¹)	R^2	K_3 (g (mg min))
		FE	0.878	0.193	0.66	0.024	0.863	0.99	0.70
MSQ	0.049	0.028	0.82	0.008	0.054	0.99	3.11	0.84	0.0045
SQ	0.013	0.003	0.26	0.015	0.013	0.99	113.95	0.49	0.0005

674

675

676

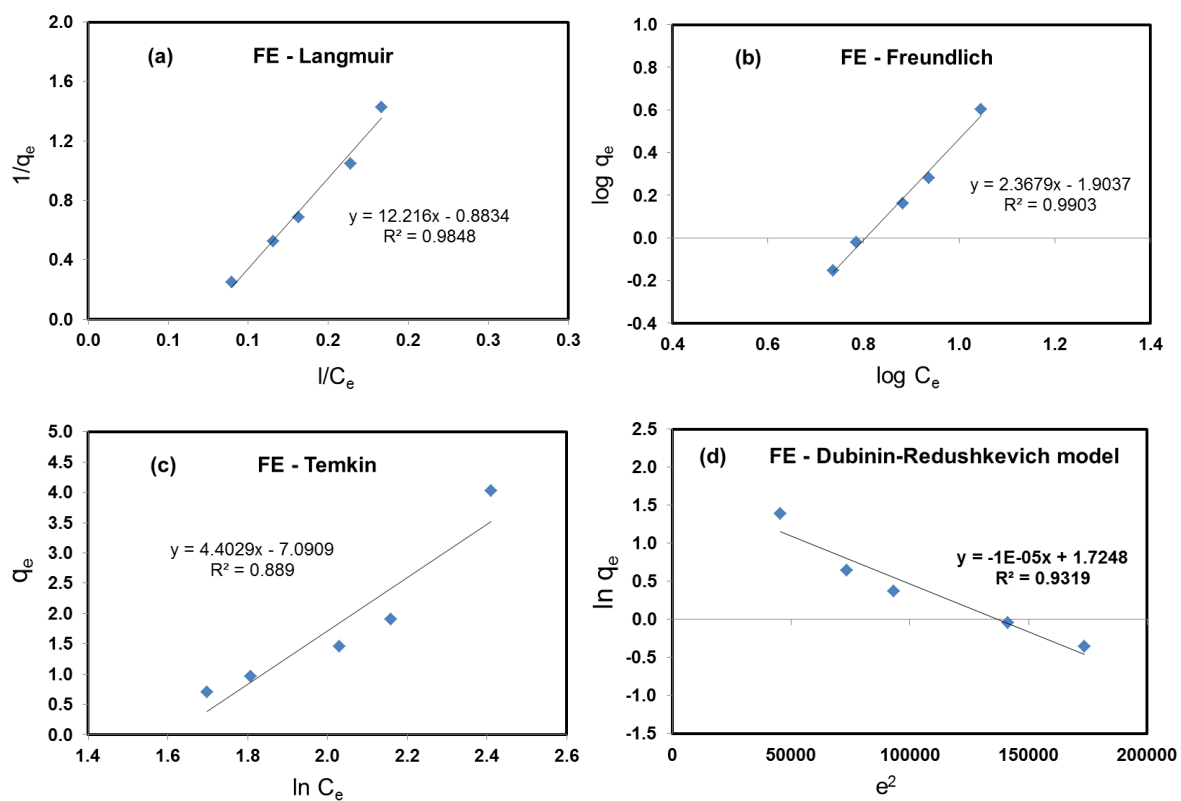
677

678

679

680 Supplementary information:

681



682

683

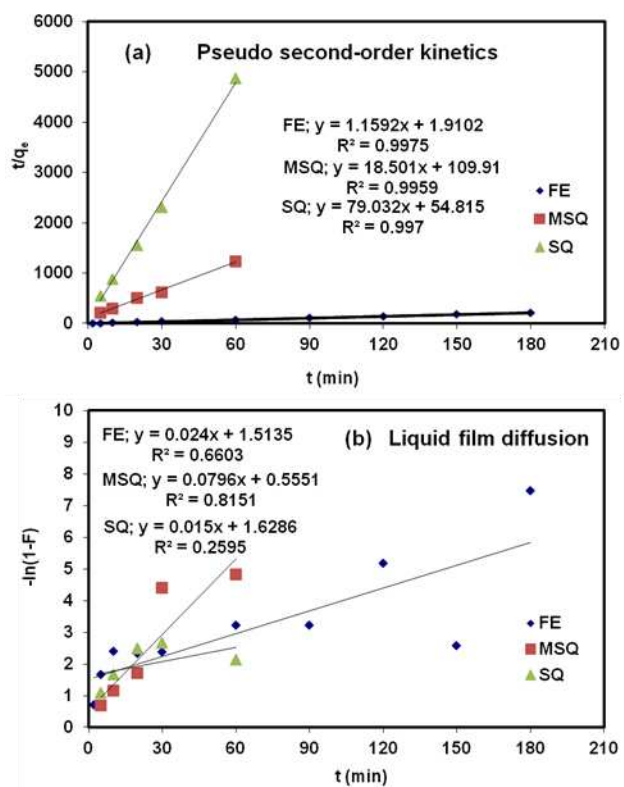
684

685 **Fig. S1.** Linear fittings of DOC adsorption on fuller's earth data to various isothermal

686 models.

687

688



689

690 **Fig. S2.** Linear fittings of DOC adsorption on fuller's earth data to (a) pseudo-second-order,
 691 and (b) liquid film diffusion models.